Limnol. Oceanogr., 55(5), 2010, 2011–2024

doi:10.4319/lo.2010.55.5.2011

The effect of CO_2 on the photosynthetic physiology of phytoplankton in the Gulf of Alaska

Brian M. Hopkinson,* Yan Xu, Dalin Shi, Patrick J. McGinn,[1] and François M. M. Morel

Department of Geosciences, Princeton University, Princeton, New Jersey

Abstract

In the high-nutrient, low-chlorophyll waters of the Gulf of Alaska, microcosm manipulation experiments were used to assess the effect of CO_2 on growth and primary production under iron-limited and iron-replete conditions. As expected, iron had a strong effect on growth and photosynthesis. A modest and variable stimulation of growth and biomass production by CO_2 (high CO_2: 77–122 Pa; low CO_2: 11–17 Pa) was observed under both iron-replete and iron-limited conditions, though near the limit of precision of our measurements in slow-growing low-iron experiments. Physiological acclimations responsible for the changes in growth were assessed. Under iron-limited conditions, growth stimulation at high CO_2 appeared to result from an increase in photosynthetic efficiency, which we attribute to energy savings from down-regulation of the carbon concentrating mechanisms. In some cases, iron-rich photosynthetic proteins (PsbA, PsaC, and cytochrome b_6) were down-regulated at elevated CO_2 in iron-limited controls. Under iron-replete conditions, there was an increase in growth rate and biomass at high CO_2 in some experiments. This increase was unexpectedly supported by reductions in cellular carbon loss, most likely decreased respiration. We speculate that this effect may be due to acclimation to decreased pH rather than high CO_2. The variability in responses to CO_2 among experiments did not appear to be caused by differences in phytoplankton community structure and may reflect the sensitivity of the net response of phytoplankton to antagonistic effects of the several parameters that co-vary with CO_2.

The concentration of CO_2 in the atmosphere is currently rising far beyond glacial–interglacial excursions of the past 800 kyr as a result of fossil fuel burning and other human activities. A portion of the anthropogenic CO_2 dissolves into seawater, altering the inorganic carbon buffer system and lowering pH. Marine organisms are expected to be affected by these chemical perturbations, called ocean acidification, through alterations of physiological processes such as calcification and photosynthesis (Riebesell et al. 2000; Beardall and Raven 2004). Variations in the concentration of CO_2 per se are presumably most relevant to autotrophic organisms, which ultimately require CO_2, and not to the more abundant bicarbonate, for fixation of carbon by the enzyme RubisCO (Cooper et al. 1969).

While the total inorganic carbon concentration in seawater is $\sim$ 2 mmol L^{-1}, the $\sim$ 10 μmol L^{-1} CO_2 in modern seawater is not sufficient to saturate carbon fixation by algal RubisCOs, which have half-saturation constants of 20–40 μmol L^{-1} CO_2 for eukaryotic microalgae and up to 750 μmol L^{-1} CO_2 for marine cyanobacteria (Badger et al. 1998; Scott et al. 2007). Consequently, many phytoplankton employ a CO_2 concentrating mechanism (CCM) to elevate the concentration of CO_2 at the site of carbon fixation, increasing the rate and efficiency of photosynthesis. Physiological work has shown that most marine phytoplankton possess a CCM, and although many of the molecular components of the CCMs remain unidentified, it appears that they are of a diverse biochemical nature (Colman and Rotatore 1995; Reinfelder et al. 2000; Badger and Price 2003). Higher oceanic CO_2 is expected to result in the down-regulation of the CCM in certain marine phytoplankton, such as diatoms and haptophytes, when external CO_2 levels approach those needed to saturate their RubisCOs (Tortell et al. 2000; Rost et al. 2003).

Down-regulation of the CCM allows energy and materials previously devoted to inorganic carbon accumulation to be reallocated. The significance of CCM down-regulation to overall cell physiology is not well constrained because the mechanistic details of phytoplankton CCMs have not been determined. However, Raven (1991) has estimated the energy expended on the CCM to be roughly 20% of the total energy used for carbon fixation. Under some conditions this energy is likely to be put toward carbon fixation and biomass production. Increased rates of photosynthesis and growth at elevated CO_2 have indeed been observed (Riebesell et al. 1993; Fu et al. 2007), most dramatically in cultures of the nitrogen-fixing cyanobacterium *Trichodesmium* (Barcelos e Ramos et al. 2007; Hutchins et al. 2007; Levitan et al. 2007). Responses that are qualitatively similar but smaller in magnitude have been observed in field assemblages in a Norwegian fjord and in the Southern Ocean (Riebesell et al. 2007; Tortell et al. 2008), but stimulation of growth and photosynthesis is not universally observed. For some organisms the energetic savings from down-regulation of the CCM may be small, and others may reallocate the energy toward alternative processes.

Under iron (Fe)–limiting conditions, which phytoplankton experience in roughly one-third of the ocean, some particular benefits of high CO_2 may occur. In order to increase growth rate when they are Fe-limited, phytoplankton must acquire Fe at a more rapid rate or use it more

* Corresponding author: bhopkins@princeton.edu

[1] Present address: Institute of Marine Biosciences, National Research Council of Canada, Halifax, Nova Scotia, Canada

Table 1. Sampling locations; initial NO_3^-, PO_4^{3-}, and Si concentrations (in μmol L^{-1}); and calculated CO_2 concentrations for high- and low-CO_2 treatments from the beginning of incubation experiments (t_0) and final time points in +Fe treatments (t_f), where CO_2 concentrations have changed most as a result of carbon fixation.

Experiment	Latitude (°N)	Longitude (°W)	NO_3^-	PO_4^{3-}	Si	Low-CO_2 t_0 (Pa)	Low-CO_2 t_f (Pa)	High-CO_2 t_0 (Pa)	High-CO_2 t_f (Pa)
1	56.17	143.83	6.6	0.64	17.8	16.7±1.0	13.3±0.4	122±10	85±9
2	58.17	147.92	9.2	1.46	10.8	12.1±0.8	11.1±0.3	77±3	74±2
3	53.66	158.00	10.0	0.89	14.3	12.1±0.4	11.8±0.3	102±8	91±2
4	58.37	148.03	7.4	0.73	11.5	14.2±0.8	14.5±0.4	78±3	73±1

efficiently (Morel 1987). The majority of Fe in phytoplankton is devoted to the photosynthetic apparatus, and so modification of this Fe pool is the most obvious way to reduce cellular Fe demand (Raven 1990; Sunda and Huntsman 1997; Strzepek and Harrison 2004). It is possible that as CO_2 rises energetic savings from down-regulation of the CCM would permit a down-regulation of the photosynthetic apparatus and, consequently, reduced cellular Fe requirements and increased growth rates in Fe-limited phytoplankton.

In this study we attempted to determine the physiological response of natural phytoplankton assemblages to elevated CO_2 under Fe-limited and Fe-replete conditions. In order to do this we conducted microcosm incubation experiments in the Gulf of Alaska, measuring ^{14}C-based gross primary production, net growth rate, and the concentration of photosynthetic proteins, among other parameters.

Methods

Experimental setup—Four experiments were conducted using water collected from within high-nutrient, low-chlorophyll (HNLC) portions of the Gulf of Alaska in August–September 2007 (Table 1). Trace metal–clean water was collected using a towed fish system in which surface seawater (1–3 m) was pumped through Teflon tubing (using a Teflon diaphragm pump) into a clean space within the ship. The clean space was constructed by walling off a portion of a room with plastic sheeting and maintaining this area at positive pressure with high-efficiency particulate-absorbing blowers. Surface seawater was collected in a 50-liter high-density polyethylene carboy (acid washed) and dispensed into acid-washed 4-liter low-density polyethylene cubitanors. Manipulations to alter CO_2 and Fe concentrations were performed (described below), and each treatment was duplicated. The bottles were sealed and placed in on-deck, flow-through incubators screened with neutral density screening to 20% of surface irradiance. Trace metal–clean procedures were used when subsampling the incubations. The outsides of the cubitanors were washed with Milli-Q water, and subsampling was done in a laminar flow hood.

Fe and CO_2 manipulations—To achieve Fe-replete conditions (+Fe treatments), 2 nmol L^{-1} additions of Fe were made from an acidified Fe-chloride stock. Fe was not added to control treatments.

CO_2 concentrations were altered via pH adjustment using Ultra-pure HCl or NaOH (Sigma Ultra). This approach was taken to minimize the potential for trace metal contamination, and in particular, dissolved inorganic carbon (DIC) was not adjusted to compensate for alkalinity changes. pH was measured using a pH electrode (Oakton pH 11 meter with Oakton 35811-71 probe) calibrated daily with National Institute of Standards and Technology pH standard buffers. Intercalibrations between the electrode measurements and spectrophotometric pH measurements using thymol blue (Zhang and Byrne 1996) were made on seawater samples to arrive at pH measurements on the total hydrogen ion scale (pH_T). The two methods differed by less than 0.1 pH units. CO_2 partial pressures were calculated based on pH_T, historical DIC concentrations in the region during the summer months (2040 ± 14 μmol L^{-1}; National Ocean Data Center: http://www.nodc.noaa.gov/), and incubation temperature (11–14°C) using equilibrium constants from Dickson and Goyet (1994), with updates to the carbonic acid equilibria, on the pH_T, from Lueker et al. (2000). By manipulating CO_2 with acid and base alkalinity was altered while total DIC was not changed (Gattuso and Lavigne 2009).

For high-CO_2 treatments approximating CO_2 levels to be reached in the next 100 yr, average pH was set between 7.58 and 7.77, corresponding to average CO_2 levels of 77–122 Pa CO_2 (Table 1). In low-CO_2 treatments approximating glacial ocean conditions, pH was set between 8.39 and 8.50, equivalent to 11–17 Pa CO_2. The CO_2 levels were chosen to represent the likely bounds of environmental CO_2 from the last glacial period to year 2100 so that any environmentally relevant responses would be elicited in these exploratory experiments. pH was monitored at each sampling. The maximal rises in pH (declines in CO_2) occurred in +Fe treatments where growth was strong (Table 1), but CO_2 levels always remained elevated well above modern values (38.5 Pa) in high-CO_2 treatments.

Biomass and nutrients—For chlorophyll *a* (Chl *a*) measurements, seawater was filtered onto GF/F filters and extracted overnight at −20°C in 90% acetone, 10% water. Chl *a* in the extract was measured fluorometrically using the method of Welschmeyer (1994). Chl *a* derived growth rates were calculated by linear regression through natural-log–transformed Chl *a* data.

Particulate organic carbon (POC) and particulate organic nitrogen (PON) were determined by combustion analysis. Water samples were filtered onto precombusted (450°C for 4 h) GF/F filters and stored at −80°C. Samples

were exposed to fuming HCl overnight to remove inorganic carbon and were then dried overnight in an oven at 60°C. Carbon content on the filter was measured by continuous flow mass spectrometry using a Eurovactor elemental analyzer and GVI Isoprime mass spectrometer (Linda Godfrey, Rutgers University). POC-based growth rates were calculated assuming exponential growth occurred between the initial and final time points (i.e., $\mu_{POC} = \ln(POC_f/POC_{init})/\Delta t$).

Macronutrients (NO_3^-, NO_2^-, PO_4^{3-}, and silicon [Si]) were measured on 0.2-μm filtered seawater samples within 24 h of collection. An autoanalyzer was used employing standard colorimetric methods (Parsons et al. 1984).

Primary production—To estimate gross primary production, 100-mL subsamples from the experiments were poured into acid-cleaned polycarbonate bottles, and 2.5–5 μCi inorganic ^{14}C was added. The bottles were placed in the same on-deck incubators in which the experiments were being conducted so that light conditions were similar to those experienced during growth. After 2–3 h, the water was filtered through a GF/F filter, which was then placed in a scintillation vial. One milliliter of 2% HCl was added to the scintillation vial and the vial was allowed to degas overnight to remove inorganic carbon. The relatively short duration of these experiments means that the carbon fixation rates approximate gross rather than net primary production. A sample (0.5 mL unfiltered water) was also taken for total ^{14}C activity, to which β-phenethylamine (0.5 mL) was added. Scintillation fluid (ScintSafe Plus 50%, Fisher Scientific) was added to the samples, and ^{14}C content was determined by liquid scintillation counting. Carbon fixation rates were determined assuming that the rate of fixation was linear over the time of incubation and that total DIC was 2040 μmol L^{-1}.

Taxonomic pigments—Taxonomically informative phytoplankton pigments were analyzed by high-pressure liquid chromatography (HPLC) using a modified version of the method described in Goericke and Montoya (1998). At the termination of experiments, water samples (~ 1 liter) were gently filtered onto GF/F filters and stored at −80°C until analyzed. Filters were extracted on ice in 1.5 mL acetone for 0.5 h, homogenized, and allowed to extract for a further 0.5 h. Following centrifugation, portions of the extract were mixed with water to produce a 60 : 40 acetone : water solution and were immediately injected into the HPLC system. Pigments were separated on a 10-cm Supelco Discovery BIO Wide Pore C8 column using a gradient between methanol : 0.5 mol L^{-1} aqueous ammonium acetate (75 : 25) and methanol. The ultraviolet and visible absorbance of pigments was used to detect the compounds in the mobile phase via a photodiode array light absorbance detector. Chromatographic peaks were identified by retention time and quantified by peak area using calibrations determined from pure pigments isolated from algal cultures.

Phytoplankton diversity—Gene sequences were obtained to assess the types of phytoplankton present in selected experimental treatments at a finer taxonomic resolution than is possible with pigments. During the final sampling of each experiment, water samples (1.5–2 liters) were filtered through 0.2-μm Sterivex filter cartridges using a peristaltic pump. The filters were flash-frozen in liquid nitrogen and stored at −80°C until processed. In an onshore laboratory the filter cartridges were broken open and the filter was divided in half. One half was saved for analysis of photosynthetic proteins (*see* below), while the second half was used to extract deoxyribonucleic acid (DNA). DNA was isolated using the Qiagen Allprep ribonucleic acid (RNA) and DNA kit, following the manufacturer's instructions, with the addition of a brief sonication step during extraction of material from the filter in lysis buffer. Nitrate reductase (NR) gene fragments of ~ 400 base pairs (bp), targeting diatoms, were amplified using the degenerate primers (forward: 5′-GRDGGHTGGTGGTACAAGCC-3′; reverse: 5′GTTGTTYMYCATBCCCAT-3′) described in Allen et al. (2005). Haptophyte organisms were targeted with primers designed to amplify portions of the 18S rRNA gene (~ 900 bp) using a universal eukaryotic forward primer (5′-ACCTGGTTGATCCTGCCAG-3′) and a haptophytes-specific degenerate reverse primer (5′-CTCGGCKRAATACGAGTGC-3′). The polymerase chain reaction (PCR) procedure used Taq polymerase with an initial denaturation at 95°C for 5 min, followed by 30 amplification cycles of 95°C for 30 s, 55°C for 30 s, and 72°C for 60 s, and a final elongation step at 72°C for 7 min. The amplified products were separated on agarose gels. A single product of the expected size was cut from the gel and purified using a Qiagen Gel Extraction kit. The PCR products were incorporated into the pGEM-T Easy vector (Promega) and cloned into JM109 competent cells following the manufacturer's instructions. Colonies were picked and screened for inserts by PCR using M13 forward and reverse primers for NR products and gene-specific primers for 18S rRNA products. PCR products were run on an agarose gel, purified using the Qiagen Gel Extraction kit, and sequenced on an Applied Biosystems Prism 3730 (Genewiz).

Experimental and reference sequences were aligned using ClustalW in MEGA4 (Tamura et al. 2007). P-distance neighbor-joining trees based on the alignments were constructed in MEGA4 and boot-strapped with 500 replicates. About half of the NR sequences obtained did not appear to be of diatom origin and were not included in the alignment or tree construction. GenBank accession numbers for the 18S rRNA sequences are GU338430-GU338454 and for the NR sequences are GU338412-GU338429.

Photosynthetic proteins—The second half of the Sterivex filter described above (*see* Phytoplankton diversity) was ripped into small pieces using sterile tweezers and placed in a 1.5-mL microcentrifuge tube. Three hundred microliters of extraction buffer (50 mmol L^{-1} Tris at pH 6.8, 2% sodium dodecyl sulfate, 10% glycerol) was added to the microcentrifuge tube, and proteins were extracted for 10 min at room temperature, with periodic vortexing. The samples were placed in near-boiling water for 5 min and

then cooled to room temperature. Filter pieces were removed and the extract was centrifuged at 10,000 × *g* for 5 min to pellet debris. Total protein concentration in the extract was determined using the bichinoninic assay (Pierce, Thermo Scientific). After the protein concentration was determined, 2% β-mercaptoethanol was added to the extract. The efficiency of protein extraction was estimated based on Chl *a* concentrations in extract, pellet, and filter fractions. The extraction efficiency was 77% ± 3% for *Thalassiosira weissflogii* cultures and 69% ± 5% for field samples.

Western blots were performed to analyze photosynthetic proteins of interest, as described in McGinn and Morel (2008). Primary antibodies targeting PsbA, cytochrome b_6 ($Ctyb_6$), and PsaC were obtained from Agrisera. For PsbA, a recombinant PsbA protein standard from *Synechocystis* PCC 6803 (Agrisera) was used for quantification. Generally, three levels of protein standard spanning the sample range were loaded. A line was fit through the standards data and used to calculate the sample abundances. Good regressions ($r^2 > 0.95$) were generally obtained. All other proteins are expressed in relative terms, but linearity of response in the Western blot was verified by serial dilution of selected samples.

The proteins analyzed are essential subunits of each of the major protein complexes involved in oxygenic photosynthesis. PsbA, also known as D1, is a core reaction center protein of PSII. The $Cytb_6$ protein is the major protein of the cytochrome b_6f complex, which is involved in electron transfer. PsaC is an electron transfer protein with 2 Fe_4S_4 Fe–sulfur clusters forming an essential component of the PSI complex.

The PsbA and PsaC antibodies are global antibodies designed against peptide tags, which are conserved across all oxygenic photosynthesizers, and so no bias in affinity of the antibody is expected, even if phytoplankton communities differ (Campbell et al. 2003). The $Cytb_6$ antibody was raised against a 14–amino acid *N*-terminal peptide conserved in *Arabidopsis thaliana* and *Chlamydomonas reinhardtii*. Although this peptide is not universally conserved, variability in this region is small among the stramenopiles (differ by one to two amino acids based on the following GenBank sequences: ABV70160, NP043648, YP874548, and YP874393) and haptophytes (differ by up to three amino acids based on the following GenBank sequence: YP277309), which dominated our experiments. Additionally, phytoplankton communities were in most cases very similar between the CO_2 treatments for which protein abundance was compared, minimizing concern about the potential of differential antibody reactivity to bias results.

Active fluorescence—A Fluorescence Induction and Relaxation Fluorometer (Satlantic) was used to measure the kinetics of chlorophyll fluorescence induction and decay with regard to the experimental phytoplankton populations. Phytoplankton samples were dark acclimated for 10–15 min prior to measurement. The measurement protocol included a single turnover phase and a multiturnover phase, although only data from the single turnover phase are analyzed here. In the single turnover phase, actinic blue light (47,000 μmol photons m^{-2} s^{-1}, centered at 450 nm) was applied continuously for 80 μs, during which fluorescence rose from its initial value (F_o) to a plateau (F_m) as a result of the closure of PSII reaction centers. Relaxation of chlorophyll fluorescence was then monitored for 135 ms to near its initial level. The multiturnover phase followed immediately, in which the actinic light was applied continuously for 40 ms, followed by relaxation of fluorescence monitored over 450 ms. Twenty to 40 replicate measurements were made on a sample and averaged. Signal from a blank, an 0.22-μm filtered sample from each treatment, was subtracted from the averaged fluorescence response.

The blank corrected fluorescence response from the single turnover phase was fitted to the Kolber et al. (1998) model of variable fluorescence using custom software. Values for F_o, F_m, and the functional absorption cross section of PSII (σ_{PSII}) were obtained from the saturation phase data. The PSII turnover time (τ), modeled as a single exponential decay function, was estimated from the relaxation of fluorescence.

Statistics—All data were assumed to be normally distributed, and so differences between means were assessed using *t*-tests. The low level of biological replication ($n = 2$) resulted in noisy responses of individual parameters, especially in Fe-limited controls, in which biomass was low. To overcome this variability, several independent parameters were examined in a single statistical test. We reasoned that several parameters (Chl *a*, POC, P, and NO_3^- drawdown) that measure very similar properties, phytoplankton biomass and production, should respond approximately proportionally to each other and so were treated as replicate measurements of a single property. The combined distribution of these parameters was considered after transformation to proportional deviations from the mean, calculated as follows:

$$y_i = \frac{x_i - \mu_x}{\mu_x} \quad (1)$$

The transformed variables should also be normally distributed under the stated assumptions, and so differences between treatments were assessed using a *t*-test (Ross 2007). The analysis was conducted to test for effects of CO_2 both in Fe-limited controls and in Fe-addition treatments and to test for the effect of Fe. The significance of these effects was assessed in individual experiments as well as in a pooled data set combining all experiments.

Results

Growth—Addition of Fe stimulated phytoplankton growth in excess of controls in experiments (expts) 1, 2, and 3, as shown by increases in Chl *a* (Fig. 1), POC (Fig. 1), and nitrate drawdown (Table 2). Growth rates calculated from Chl *a* and POC data, assuming exponential growth, also showed increases under Fe-replete conditions (Table 3). This response was expected, since the Gulf of

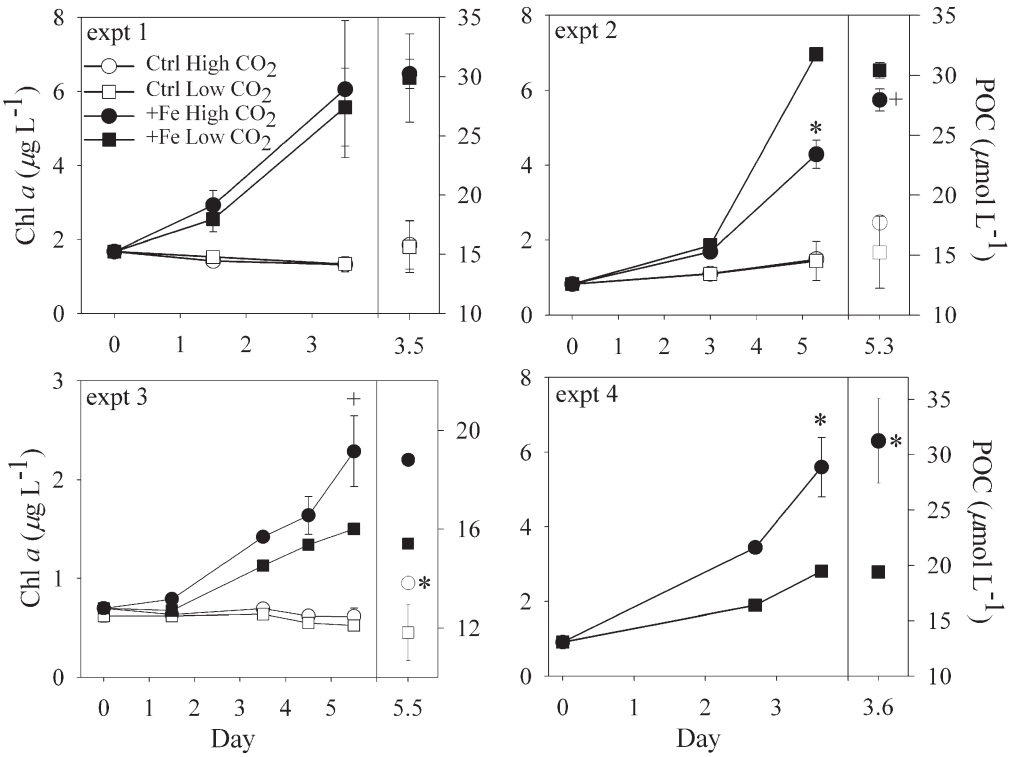

Fig. 1. Chl *a* and POC data from the Fe- and CO_2-manipulation experiments. The time course data are Chl *a* concentrations from each point at which the experiments were sampled. POC data from the final time point are plotted on the right in each panel. All data are averages of duplicate bottles, and error bars represent the standard deviation between replicates, except the POC data for expt 3 +Fe–high CO_2, which are from a single bottle only. Differences between CO_2 treatments were assessed at the final time point using *t*-tests; *t*-tests between CO_2 treatments with *p*-values < 0.1 are indicated with a plus sign (+), and those with *p*-values < 0.05 are indicated with an asterisk (*).

Alaska is a classic Fe-limited, HNLC region (Martin and Fitzwater 1988).

Under Fe-limiting conditions, CO_2 had little effect on Chl *a* (Fig. 1), nutrient drawdown, or growth rates in individual experiments (Tables 2, 3). A significant increase in POC at high CO_2 was observed in expt 3. Under Fe-replete conditions, however, high CO_2 significantly stimulated growth rates and nitrate drawdown in expt 4 and enhanced Chl *a* accumulation and POC production in expts 3 and 4 (Fig. 1). Time course data for Chl *a* show that these differences developed early and were maintained or increased as the experiment progressed (Fig. 1). By the end of expt 2, Chl *a* was lower at high CO_2 in +Fe treatments. This was predominantly due to a change in the Chl *a*:C ratio (discussed below), since POC levels were similar in the two CO_2 treatments and nitrate drawdown was only slightly higher at low CO_2.

A set of biomass (Chl *a*, POC) and production (P, NO_3^- drawdown) parameters expected to covary proportionally were examined jointly to increase statistical power (Table 4). This analysis confirmed the effects of Fe and the effects of CO_2 in +Fe treatments, which were evident from analysis of individual parameters. A positive effect of CO_2 in Fe-limited controls is seen in the data pooled from all experiments. This effect is primarily due to the contributions from expt 3, though expt 2 also contributes and nearly has a significant CO_2 effect on its own.

Primary production—In response to added Fe, ^{14}C-based gross primary production per unit volume of medium (P) increased in all experiments, although chlorophyll normalized rates (P^B) were variable (Table 2). Other investigators (Hiscock et al. 2008) also have noted variability in the response of P^B to Fe addition, with increases observed on some occasions, as in expt 1, or with no effect, as in expt 2. A decline in P^B in Fe-replete treatments was seen in expt 3. No significant differences in P^B between CO_2 treatments were found, except for a slight increase in P^B in +Fe–high CO_2 treatment in expt 2 (Table 2).

Photosynthetic physiology—We examined the effects of Fe and CO_2 on key photosynthetic proteins that reflect the abundance of Photosystem II (PsbA), Photosystem I (PsaC), and the cytochrome b_6f complex ($Cytb_6$). Down-regulation of photosynthetic proteins is expected in Fe-limited conditions (Strzepek and Harrison 2004). Photosynthetic proteins were indeed present in much greater abundance in +Fe treatments compared to Fe-limited controls (Fig. 2). However, because the data are normalized to total protein, a larger increase in autotrophs (which contribute photosynthetic proteins) compared to heterotrophs (which contribute only to the total protein) in the +Fe treatments likely exaggerates this difference.

A nearly 50% reduction in the abundance of all three photosynthetic proteins was seen in the +Fe treatments of

Table 2. Biomass and production measurements from the final time point of each experiment. Data for Chl *a* (μg L^{-1}), particulate organic carbon (POC, μmol L^{-1}), ^{14}C-based gross primary production (P, μmol C L^{-1} h^{-1}), Chl *a*–normalized primary production (P^B, μmol C μg Chl^{-1} h^{-1}), and NO_3^- drawdown (μmol L^{-1}) between the initial and final time points are presented as average ± standard deviation between duplicate bottles. Differences between low (L)– and high (H)–CO_2 treatments were assessed with *t*-tests. A *p*-value < 0.1 is indicated with a parenthetical plus symbol (+), and *p*-values of < 0.05 are indicated with an asterisk (*). Missing data (no data), nd.

		Chl *a*		POC		P		P^B		NO_3^- drawdown	
Expt	C or +Fe	L CO_2	H CO_2	L CO_2	H CO_2	L CO_2	H CO_2	L CO_2	H CO_2	L CO_2	H CO_2
1	Control	1.33±0.04	1.33±0.20	15.6±2.1	15.8±2.0	0.12±0.04	0.12±0.04	0.087±0.023	0.095±0.017	0.7±0.3	0.7±0.2
1	+Fe	5.57±1.05	6.06±1.84	29.9±3.7	30.2±1.2	1.69±0.34	1.87±0.61	0.293±0.033	0.292±0.054	5.3±0.9	5.7±1.2
2	Control	1.44±0.52	1.49±0.07	15.2±3.0	17.7±0.1	0.20±0.07	0.38±0.20	0.140±0.003	0.262±0.170	1.5±0.5	1.7±0.0
2	+Fe	6.96±0.15	4.28*±0.37	27.9±0.9	30.4(+)±0.7	1.30±0.06	0.89*±0.10	0.187±0.005	0.207*±0.004	7.1±0.2	6.2*±0.1
3	Control	0.52±0.03	0.62±0.08	11.8±1.1	13.8*±0.1	0.14±0.01	0.19*±0.02	0.260±0.000	0.328±0.048	nd	nd
3	+Fe	1.50±0.05	2.29(+)±0.35	15.4±0.0	18.8	0.35±0.02	0.58*±0.04	0.243±0.011	0.250±0.027	nd	nd
4	+Fe	2.80±0.11	5.60*±0.79	19.4±0.3	31.3*±3.8	0.62±0.01	1.22*±0.09	0.222±0.005	0.221±0.047	1.6±0.2	3.2*±0.1

expt 2 at high CO_2 compared to low CO_2 (Fig. 2). The concomitant reduction in Chl *a*:POC ratios presumably indicates that fewer photosynthetic units per cell were produced at elevated CO_2 (Fig. 1). In all other experiments, photosynthetic protein abundance was unaffected by CO_2 under Fe-replete conditions (Fig. 2). However, it is notable that in expts 3 and 4 higher growth rates were achieved at high CO_2 despite constant levels of P^B and photosynthetic proteins.

In expts 1 and 3, in Fe-limited controls, PsbA and $Cytb_6$ were reduced at high CO_2 (50% in expt 1 and 10–20% in expt 3; Fig. 2). The abundance of PsaC was too low to be detected in protein extracts from control treatments, which is likely the result of low biomass and down-regulation of this Fe-rich protein under Fe-limited conditions (Strzepek and Harrison 2004). In expt 3, the reduction in photosynthetic proteins was associated with a drop in Chl *a*:POC (Fig. 1).

As expected, Fe availability influenced variable fluorescence parameters ($F_v:F_m$, σ_{PSII}, τ) with increases in $F_v:F_m$ under Fe-replete conditions being the most notable and consistent effect (Table 5). There were only a few significant effects of CO_2 treatments on $F_v:F_m$ (Table 5) and no significant effects of CO_2 on σ_{PSII} or τ (data not shown). In expts 2 and 3, $F_v:F_m$ was slightly higher in the +Fe–high CO_2 treatment relative to the low-CO_2 treatment. In contrast, in expt 3 a slight reduction in $F_v:F_m$ was observed at high CO_2 under Fe limitation. None of these effects are likely to be physiologically significant.

Phytoplankton community structure—Pigment signatures indicate that initial phytoplankton communities in expts 1, 2, and 4 were dominated by haptophytes, with pelagophytes, diatoms, and chlorophytes all contributing substantially to the total biomass, while in expt 3 haptophytes and chlorophytes were equally dominant (Fig. 3). In all experiments, diatoms and haptophytes responded most strongly to Fe additions, while pelagophytes and chlorophytes showed minimal increases. Such responses have been seen in previous experiments and are attributed to the ability of larger phytoplankton to grow more rapidly than their grazers once Fe limitation is relieved (Landry et al. 2000; de Baar et al. 2005).

CO_2 levels also altered pigment concentrations in the +Fe treatments of expts 2, 3, and 4, but did not do so in controls (Fig. 3). In expt 2, the observed decrease in 19-hexanoyloxyfucoxanthin (19-hex) and fucoxanthin (fucox) at high Fe and CO_2 probably resulted not from a difference in community structure but from down-regulation of the photosynthetic apparatus in selected taxa, as indicated by decreases in Chl *a*:POC ratio and photosynthetic proteins. The affected taxa may have been haptophytes alone (which commonly contain both 19-hex and fucox; Jeffrey and Wright 1994) or both diatoms (fucox only) and haptophytes. In expts 3 and 4, the much greater increase in fucox than in Chl *b* in the +Fe–high CO_2 treatment demonstrates that the bulk of the increase in phytoplankton growth rate and biomass in these samples can be attributed to diatoms.

To better assess the identity of phytoplankton in +Fe treatments, we analyzed gene sequences diagnostic of diatoms (NR) and haptophytes (18S rRNA), the two taxa that dominated biomass in +Fe treatments. Haptophyte

Table 3. Chl *a*–based growth rates (μ_{Chl}, d^{-1}) were calculated by linear regression through natural-log–transformed Chl *a* data. Errors represent standard errors in the slope, and CO_2 treatments with non-overlapping 95% confidence intervals are indicated with an asterisk (*). POC-based growth rates (μ_{POC}, d^{-1}), calculated assuming exponential growth between the initial and final time points, are presented as average ± standard deviation between duplicate bottles. Significant differences in μ_{POC} between CO_2 treatments were assessed with a *t*-test. *p*-values < 0.05 are indicated with an asterisk (*).

		μ_{Chl}		μ_{POC}	
Expt	Treatment	Low CO_2	High CO_2	Low CO_2	High CO_2
1	Control	−0.06±0.00	−0.06±0.02	0.00±0.04	−0.02±0.05
1	+Fe	0.35±0.03	0.37±0.00	0.21±0.04	0.25±0.06
2	Control	0.10±0.01	0.10±0.01	0.05±0.04	0.08±0.00
2	+Fe	0.39±0.08	0.31±0.04	0.18±0.00	0.17±0.01
3	Control	−0.02±0.00	−0.02±0.01	0.02±0.01	0.06±0.00
3	+Fe	0.16±0.02	0.22±0.02	0.08±0.00	0.11
4	+Fe	0.30±0.03	0.50*±0.00	0.15±0.00	0.28*±0.03

18S rRNA sequences fall into two clusters (Fig. 4): one with high identity to sequences from *Emiliania huxleyi* and *Gephyrocapsa oceanica* (Noelaerhabdaceae), the second closely related to sequences from *Phaeocystis* spp. (Saez et al. 2004). Despite the limited numbers of sequences, it appears that the haptophyte communities in expts 2 and 3 were similar and belonged to both the Noelaerhabdaceae and Phaeocystales, while in expt 1 they belonged chiefly to the Phaeocystales, and in expt 4 they belonged primarily to the Noelaerhabdaceae. The diatom NR sequences also fall into two clusters, but the lack of appropriate reference sequences, particularly for pennate diatoms, prevents taxonomic identification (Fig. 5). Nonetheless, the results indicate that the diatom assemblages in expts 1, 2, and 4 were quite similar. Only one NR sequence from expt 3 appeared to be of diatom origin. Other NR sequences were derived from haptophytes and green algae.

Discussion

The CO_2- and Fe-manipulation experiments we conducted were designed to assess potential changes in phytoplankton growth and physiology resulting from environmental CO_2 variability. Fe clearly had the largest effect on phytoplankton, increasing biomass and production parameters by an average 2.2-fold measure (Table 4). CO_2 had a secondary effect on biomass and production that was positive overall but variable. The same biomass and production parameters increased at high CO_2 by an average of 17% in Fe-limited controls and by an average of 20% in Fe-addition treatments. The effect of CO_2 under Fe limitation may have been due to energetic savings from down-regulation of the CCM, allowing increased efficiency of carbon fixation and, in some cases, the reduction of Fe-rich photosynthetic proteins. In Fe-replete treatments, elevated CO_2 increased growth by lowering carbon losses, most likely as a result of reduced respiration.

Table 4. Results of a statistical analysis of a set of biomass (Chl *a*, POC) and production parameters (P, NO_3^- drawdown). *p*-values based on *t*-tests are presented for the individual experiments and the combined data from all experiments. The direction and magnitude of the tested effects are indicated by the parameter z, which is the average fractional difference between high-CO_2 and low-CO_2 parameter values in CO_2 effect analyses and +Fe and controls in the Fe effect analysis (for example: parameter values are, on average, 17% higher in the high-CO_2 controls compared to low-CO_2 controls of expt 3).

	CO_2 effect in controls		CO_2 effect in +Fe		Fe effect	
Expt	*p*	z	*p*	z	*p*	z
1	0.44	0.08	0.21	0.10	<0.001	3.84
2	0.13	0.27	<0.001	−0.24	<0.001	2.10
3	<0.01	0.17	<0.001	0.42	<0.001	1.27
4			<0.001	0.89	—	—
All	0.02	0.17	<0.001	0.20	<0.001	2.26

Effect of CO_2 in Fe-limited controls—A positive effect of CO_2 on Fe-limited phytoplankton was hypothesized to occur as a result of energetic savings from the CCM. The average effect we saw was relatively weak (17% increase of several parameters) and near the limit of precision of our measurements in slow-growing control experiments (Table 4). A portion of photosynthetic energy (in the form of adenosine triphosphate and nicotinamide adenine dinucleotide phosphate) is generally used to power the CCM (Sultemeyer et al. 1991; Kaplan and Reinhold 1999). In Fe-limited phytoplankton, which are effectively energy limited (Sunda and Huntsman 1997), an increased efficiency of carbon fixation per unit of light absorbed (for which P^B is a proxy) would thus be expected at elevated CO_2 if energy from CCM down-regulation is directed to carbon fixation. Although P^B increased at high CO_2 in Fe-limited controls in all experiments, the difference is not statistically significant in any single experiment (Table 2). Analyzing these P^B data together using the statistical procedure described in the methods shows that the effect of CO_2 on P^B under Fe limitation in all experiments is significant only at $p = 0.11$.

In some cases energetic savings from down-regulation of the CCM at elevated CO_2 may allow Fe-limited phytoplankton to down-regulate Fe-rich photosynthetic proteins. We observed such a response in two experiments (Fig. 2).

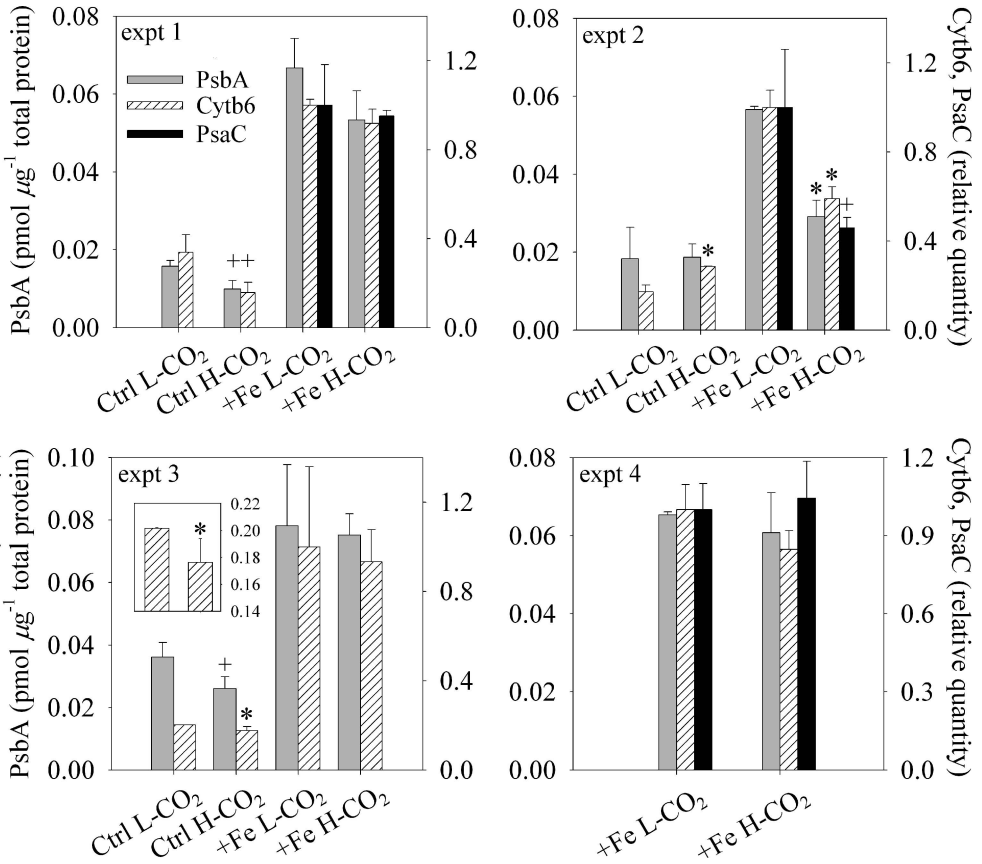

Fig. 2. Photosynthetic protein abundances from the final time point of each experiment. PsbA was quantified using protein standards, while $Cytb_6$ and PsaC are relative quantities normalized in each experiment to values in the +Fe–low CO_2 treatment. The inset in the panel showing expt 3 replots the $Cytb_6$ data from the control treatments to show the effect of CO_2. We were unable to measure PsaC in expt 3. L-CO_2 indicates low-CO_2 treatment (11.1–16.7 Pa), and H-CO_2 indicates the high-CO_2 treatment (73–122 Pa). Values are the averages from duplicate bottles, and error bars represent standard deviations between replicate bottles. *t*-tests between CO_2 treatments with *p*-values < 0.1 are indicated with a plus sign (+), and those with *p*-values < 0.05 are indicated with an asterisk (*).

Given that photosynthetic proteins appear to account for most of the Fe requirement of Fe-limited phytoplankton (Sunda and Huntsman 1997; Strzepek and Harrison 2004), the down-regulation of the photosynthetic apparatus at high CO_2 would be expected to result in lower Fe quotas, allowing increased growth. Direct measurements of Fe quotas, especially at the cellular level, would help support this provisional conclusion (Twining et al. 2004).

In summary, there is some evidence to support the hypotheses that elevated CO_2 benefits Fe-limited phytoplankton by increasing the efficiency of carbon fixation and/or reducing Fe quotas, but the effects are variable and in some cases of marginal statistical significance. The positive effects of elevated CO_2 may be moderated by reduced Fe bioavailability due to a greater extent of complexation by organic ligands at low pH (high CO_2) (Shi et al. 2010).

Reduced cellular carbon loss at high CO_2—Under Fe-replete conditions, photosynthetic efficiency (P^B) remained remarkably constant between high- and low-CO_2 treatments in all experiments except expt 2 (*see* below). Nonetheless, growth clearly increased in two experiments at high CO_2. The increased growth rates were linked to reductions in cellular carbon losses, most likely a decreased respiration rate. To explain these results it is helpful to

Table 5. $F_v : F_m$ at the final time point in each experiment presented as average ± standard deviation. *t*-tests between CO_2 treatments with *p*-values < 0.1 are indicated with a parenthetical plus sign (+), and those with *p*-values of < 0.05 are indicated with an asterisk (*).

Experiment, treatment	Low CO_2	High CO_2
1, control	0.18±0.02	0.20±0.03
1, +Fe	0.34±0.01	0.35±0.02
2, control	0.12±0.03	0.17±0.06
2, +Fe	0.29±0.01	0.33±0.01(+)
3, control	0.26±0.01	0.23±0.01(+)
3, +Fe	0.41±0.01	0.44±0.00*
4, +Fe	0.47±0.02	0.49±0.03

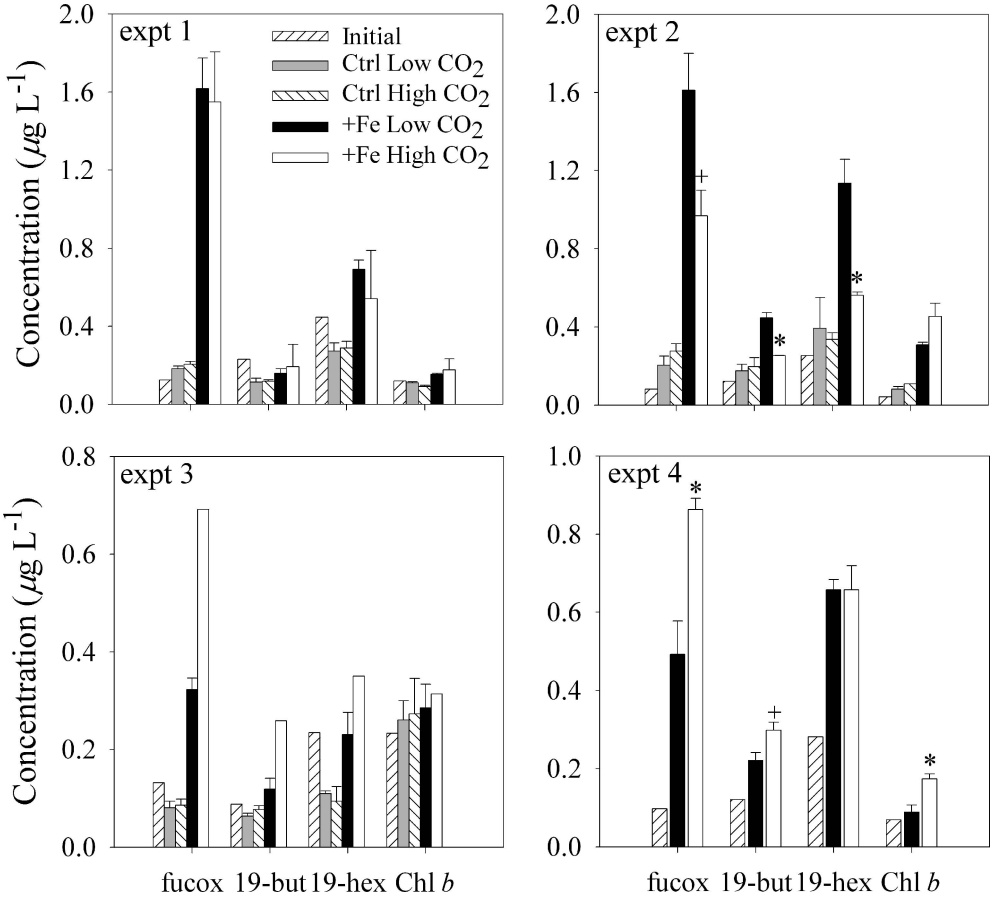

Fig. 3. Phytoplankton pigment concentrations from experiments at the initial and final time points. Pigments are derived from the following taxa: fucox: diatoms, prymnesiophytes; 19-but: pelagophytes, prymnesiophytes; 19-hex: prymnesiophytes; Chl *b*: chlorophytes. Final time-point data are the averages from duplicate bottles, and error bars represent standard deviations between replicate bottles, except for expt 3 +Fe–high CO_2, from which data were only obtained from a single replicate. Initial data are from a single sample. *t*-tests between CO_2 treatments with *p*-values < 0.1 are indicated with a plus sign (+), and those with *p*-values < 0.05 are indicated with an asterisk (*).

consider the following approximation for growth rate:

$$\mu = \frac{P^B \times \text{Chl } a - L}{POC} \quad (2)$$

with P^B in μmol (μg Chl *a*)$^{-1}$ d^{-1}, calculated from ^{14}C fixation rates and hours of sunlight per day; Chl *a* in μg L^{-1}; L representing an unmeasured carbon loss term (respiration, dissolved organic carbon [DOC] excretion, grazing, etc.); and POC (in μmol L^{-1}) being an approximation of phytoplankton biomass.

In two experiments (expts 3 and 4) higher growth rates and/or carbon biomass production were observed at elevated CO_2 under Fe-replete conditions. In expts 3 and 4 this higher growth rate was achieved despite a lack of difference in P^B values between treatments (Table 2). In expt 4, Chl *a*:POC ratios were higher at elevated CO_2 (Table 2), but the 1.2× difference in Chl *a*:POC is not sufficient to fully explain the 1.67× elevation in Chl *a*–derived growth rate at high CO_2 (Table 3). A similar response to CO_2 was seen in the +Fe treatments of expt 3. Consequently, lower loss rates at high CO_2 are expected to account for the remaining difference in growth rate and carbon biomass production. Tortell et al. (2008) made a similar observation in experiments from the Southern Ocean, where carbon fixation rates declined relative to growth rates at high CO_2.

Of the possible mechanisms for alteration of the carbon loss term, differences in respiration rates seem most reasonable. Excretion of DOC has generally been found to be greater at high CO_2 (Engel et al. 2004), and there is no reason to expect grazing pressure to differ between CO_2 treatments. Respiration, on the other hand, may decline as a result of reduced energy expenditure on intracellular pH homeostasis or the CCM. We had hypothesized that energetic savings at high CO_2 would result from CCM down-regulation. The CCM is powered by respiration in some organisms, but this is unusual (Huertas et al. 2002). Instead, respiration may decrease at low ambient pH because of declines in energy expenditure on pH homeo-

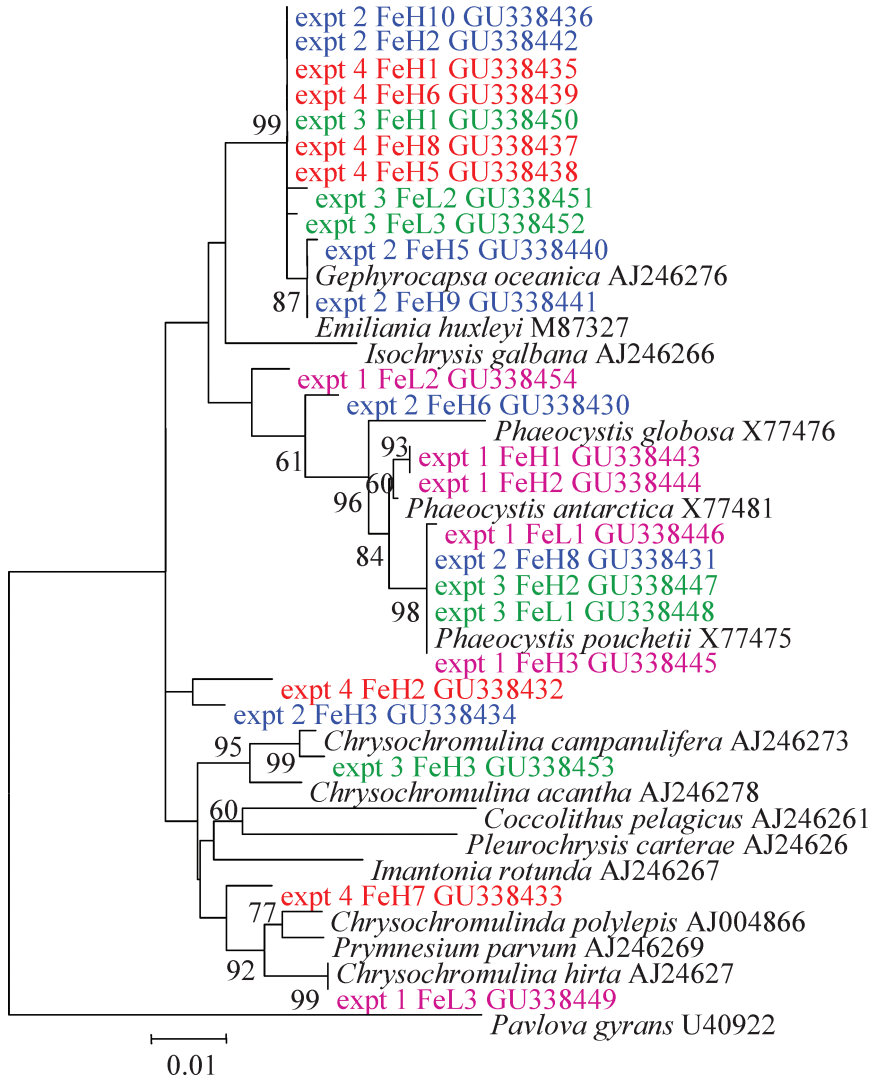

Fig. 4. A phylogenetic tree of haptophyte 18S rRNA sequences from the experiments. The tree is a consensus p-distance tree built by neighbor-joining methods in MEGA4. The tree was rooted using the 18S rRNA sequence of *Pavlova gyrans*. The experiment, treatment (all from +Fe treatment, L indicates low CO_2, H indicates high CO_2), and GenBank accession numbers are indicated for each sequence on the tree. The sequences are color-coded by experiment. Reference sequences from cultured organisms are included. Five hundred bootstrap replicates were performed, and branches with support in $> 60\%$ of these trees are indicated with the percent support on the tree. The scale bar indicates the fraction of differences per site.

stasis. The cytosol is actively maintained at a pH of $\sim$ 7.0–7.5, and so as external pH nears the desired intracellular pH, less energy may be needed for pH homeostasis (Anning et al. 1996). Such a savings may or may not occur depending on how a cell adjusts its transmembrane electrical potential to support its cation motive forces in response to a change in ambient pH (Smith and Raven 1979).

In an alternative response to CO_2, a down-regulation of the photosynthetic apparatus at high CO_2 was observed in expt 2, as indicated by decreased abundances of photosynthetic proteins and lowered Chl *a* : POC ratios (Figs. 1, 2). Equation 2 implies that the net effect of differences in P^B and Chl *a* : POC would be a 0.8$\times$ reduction in growth rate at high CO_2 if loss rates were constant. However, POC-based growth rate and nutrient drawdown were similar in the two CO_2 treatments, implying that loss rates, most likely respiration, must again have decreased at high CO_2. Such a down-regulation of the photosynthetic machinery at high CO_2 is, however, surprising. The interpretation of results from microcosm experiments that include heterotrophs as well as autotrophs is fraught with difficulties. We cannot rule out the possibility that both high-CO_2 bottles fortuitously contained more grazers than the low-CO_2 treatments. It is also possible that the CO_2–pH effect results from a change in availability of some other micronutrient. In any case, the results for expt 2 under Fe-replete conditions are clearly in contrast to those of the other experiments.

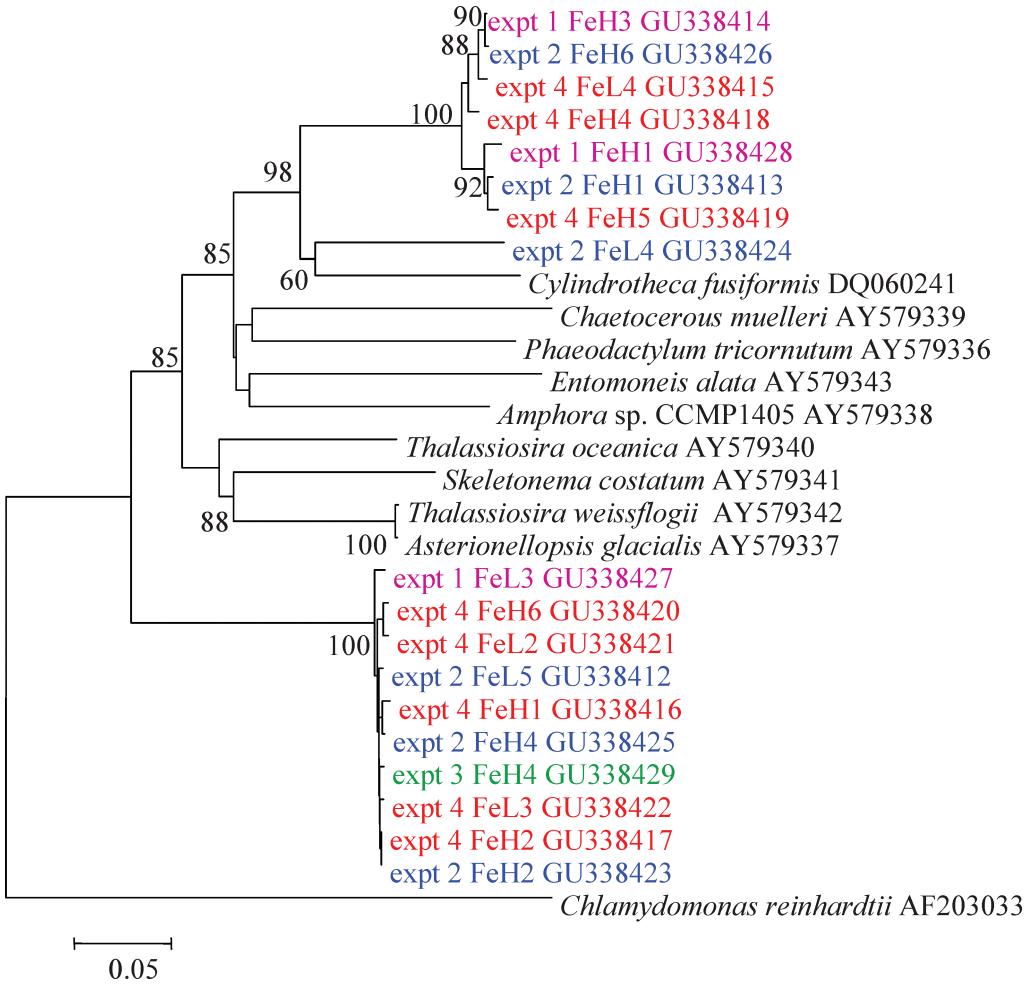

Fig. 5. A phylogenetic tree of diatom NR sequences from the experiments. The tree is a consensus p-distance tree built by neighbor-joining methods in MEGA4 and was rooted with the NR sequence from *Chlamydomonas reinhardtii*. The experiment, treatment (all from +Fe treatment, L indicates low CO_2, H indicates high CO_2), and GenBank accession numbers are indicated for each sequence on the tree. The sequences are color-coded by experiment. Reference sequences from cultured organisms are included. Five hundred bootstrap replicates were performed, and branches with support in $> 60\%$ of these trees are indicated with the percent support on the tree. Scale bar indicates the fraction of differences per site.

Variability in response to CO_2—Unlike the response of ambient phytoplankton to Fe, responses to CO_2 treatments varied significantly among experiments, as other investigators have observed in both laboratory and field experiments (Burkhardt et al. 1999; Tortell et al. 2008). Such variability may be caused by differences in phytoplankton community structure. Various studies (Badger et al. 1998; Burkhardt et al. 1999; Riebesell et al. 2000) have shown the physiological effects of CO_2 to be species specific, and CCMs likely differ among phytoplankton taxa. However, there is no obvious relationship between the community structure of a given incubation and the response to CO_2. Pigment data suggest that initial communities were generally similar and that phytoplankton community structure in control treatments did not change greatly from the initial conditions (Fig. 3). In Fe-replete treatments the genetic data show diatom taxa were similar in all experiments, yet different responses to elevated CO_2 were seen (Fig. 5). Haptophyte organisms were different in several experiments, but there is no clear relationship between the taxa present and the response to CO_2 observed (Fig. 4).

Other explanations for the differential responses are speculative. It is possible that the parameters altered along with CO_2 have differing, potentially antagonistic, effects on components of the phytoplankton community. For example, in an acidified treatment, higher CO_2 may allow down-regulation of the CCM, but reduced CO_3^{2-} may inhibit calcification of coccolithophores, increasing their susceptibility to grazing, or lowered pH may reduce Fe bioavailability (Shi et al. 2010). The net result of these effects on parameters such as community growth rate and biomass may be quite sensitive to the combination of environmental conditions. The unraveling of these effects may necessitate measurement of additional oceanographic or physiological properties, such as CCM characteristics, calcification rates, trace metal concentrations, or history of the water mass (for example, light availability, mixed layer depth, or Fe supply).

Time-scale considerations—The response of phytoplankton physiology to changes in CO_2 includes both transient responses and long-term acclimations. Based on chlorophyll-derived growth rates (Table 3), phytoplankton in Fe-replete treatments produced, on average, 2.0 ± 0.5 (range 1.2–3.0) subsequent generations. This is likely sufficient time for acclimation to both CO_2 and, of course, Fe, as is evident from the response of PSII fluorescence parameters and photosynthetic proteins to Fe addition. In contrast, under Fe-limited conditions minimal growth rates based on POC turnover, calculated from POC concentrations and ^{14}C primary production (Table 2), in Fe-limited treatments indicate that an average 1.0 ± 0.7 (range 0.5–2.0) subsequent generations experienced the altered CO_2 conditions. The duration of the experiment may not have been sufficient for full acclimation of the very slow-growing cells to CO_2 treatments, and so some effects of CO_2 may not have been observed.

Consequences for the ocean—Our results provide evidence for an expected increase in photosynthetic efficiency at high CO_2 under Fe-limited (and thus energy-limited) conditions, although the data are noisy. We also inferred a surprising but highly significant decrease in carbon loss, most likely reduced respiration, at high CO_2 under nutrient-replete conditions. This led to increased growth rates at elevated CO_2 in two experiments, implying that populations of nutrient-replete phytoplankton in the field may also grow faster at elevated CO_2. Although the precise cause of this effect is not clear, it is possible that N- and P-limited phytoplankton may be affected similarly, since they are also not limited in the energy they can devote to operating a CCM.

Increased photosynthetic efficiency and lowered Fe quotas should allow phytoplankton in Fe-limited waters to grow more rapidly and to attain higher biomass at elevated CO_2. However, because our experiments did not include a modern CO_2 treatment, it is not possible to determine to what extent Fe-limited phytoplankton will be affected by CO_2 increases over the next century. Culture studies (Shi et al. 2010) on Fe-limited diatoms indicate that most of the effects of CO_2 occur below ambient or preindustrial levels.

To predict the net effect of climate change on growth and biomass in Fe-limited regions will also require knowledge of changes in Fe supply and bioavailability. Dust deposition and riverine inputs of Fe may be altered through changes in the hydrologic cycle. Fe speciation and consequently bioavailability will also be affected by changes in pH-dependent factors, including Fe(II) lifetime, organic complexation, and Fe–oxyhydroxide solubility (Shi et al. 2010). The combined effects of changes in Fe quotas, Fe use efficiency, and Fe availability will ultimately determine how production and biomass will be altered by rising CO_2 in Fe-limited portions of the ocean.

Acknowledgments

We thank Ken Bruland, chief scientist of the Gulf of Alaska cruise, for allowing us to participate in the cruise and for providing access to trace metal–clean water and Bettina Sohst for nutrient analyses. We also thank the captain and crew of the R/V *Thomas G. Thompson* for their assistance. Bess Ward provided advice on the use of nitrate reductase as a phylogenetic marker in diatoms. Fredrik Simons assisted with statistical analyses. We thank two anonymous reviewers for helpful comments and careful analysis of the article. This work was funded by the National Science Foundation and by a grant to the Princeton Environmental Institute from British Petroleum and Ford Motor Co.

References

Allen, A. E., B. B. Ward, and B. Song. 2005. Characterization of diatom (Bacillariophyceae) nitrate reductase genes and their detection in marine phytoplankton communities. J. Phycol. **41:** 95–104, doi:10.1111/j.1529-8817.2005.04090.x

Anning, T., N. Nimer, M. J. Merret, and C. Brownlee. 1996. Costs and benefits of calcification in coccolithophorids. J. Mar. Syst. **9:** 45–56, doi:10.1016/0924-7963(96)00015-2

Badger, M. R., T. J. Andrews, S. M. Whitney, M. Ludwig, D. C. Yellowlees, W. Leggat, and G. D. Price. 1998. The diversity and coevolution of RubisCO, plastids, pyrenoids, and chloroplast-based CO_2 concentrating mechanisms in algae. Can. J. Bot. **76:** 1052–1071, doi:10.1139/cjb-76-6-1052

———, and G. D. Price. 2003. CO_2 concentrating mechanisms in cyanobacteria: Molecular components, their diversity and evolution. J. Exp. Bot. **54:** 609–622, doi:10.1093/jxb/erg076

Barcelos e Ramos, J., H. Biswas, K. G. Schulz, J. LaRoche, and U. Riebesell. 2007. Effect of rising atmospheric carbon dioxide on the marine nitrogen fixer *Trichodesmium*. Glob. Biogeochem. Cycles **21:** GB2028, doi:10.1029/2006GB002898

Beardall, J., and J. A. Raven. 2004. The potential effects of global climate changes on microalgal photosynthesis, growth and ecology. Phycologia **43:** 26–40, doi:10.2216/i0031-8884-43-1-26.1

Burkhardt, S., I. Zondervan, and U. Riebesell. 1999. Effect of CO_2 on C:N:P ratio in marine phytoplankton: A species comparison. Limnol. Oceanogr. **44:** 683–690, doi:10.4319/lo.1999.44.3.0683

Campbell, D. A., A. M. Cockshutt, and J. Porankiewicz-Asplund. 2003. Analyzing photosynthetic complexes in uncharacterized species or mixed microalgal communities using global antibodies. Physiol. Plant. **119:** 322–327, doi:10.1034/j.1399-3054.2003.00175.x

Colman, B., and C. Rotatore. 1995. Photosynthetic inorganic carbon uptake and accumulation in two marine diatoms. Plant Cell Environ. **18:** 919–924, doi:10.1111/j.1365-3040.1995.tb00601.x

Cooper, T. G., D. Filmer, M. Wishnick, and M. D. Lane. 1969. The active species of CO_2 utilized by ribulose diphosphate carboxylase. J. Biol. Chem. **244:** 1081–1083.

de Baar, H. J. W., and others. 2005. Synthesis of iron fertilization experiments: From the iron age to the age of enlightenment. J. Geophys. Res. **110:** C09S16, doi:10.1029/2004JC002601

Dickson, A. G. and C. Goyet [eds.]. 1994. DOE handbook of methods for the analysis of the various parameters of the carbon dioxide system in sea water. Version 2. ORNL/CDIAC-74.

Engel, A., D. Delille, S. Jacquet, U. Riebesell, E. Rochelle-Newall, A. Terbrugeen, and I. Zondervan. 2004. TEP and DOC production by *Emiliania huxleyi* exposed to different CO_2 concentrations: A mesocosm experiment. Aquat. Microb. Ecol. **34:** 93–104, doi:10.3354/ame034093

Fu, F. X., M. E. Warner, Y. Zhang, Y. Feng, and D. A. Hutchins. 2007. Effects of increased temperature and CO_2 on photosynthesis, growth, and elemental ratios in marine *Synechococcus* and *Prochlorococcus* (cyanobacteria). J. Phycol. **43:** 485–496, doi:10.1111/j.1529-8817.2007.00355.x

Gattuso, J. P., and H. Lavigne. 2009. Technical note: Approaches and software tools to investigate the impact of ocean acidification. Biogeosciences **6:** 2121–2133, doi:10.5194/bg-6-2121-2009

Goericke, R., and J. P. Montoya. 1998. Estimating the contribution of microalgal taxa to chlorophyll *a* in the field—variations of pigment ratios under nutrient- and light-limited growth. Mar. Ecol. Prog. Ser. **169:** 97–112, doi:10.3354/meps169097

Hiscock, M. R., and others. 2008. Photosynthetic maximum quantum yield increases area, an essential component of the Southern Ocean phytoplankton response to iron. Proc. Natl. Acad. Sci. USA **105:** 4775–4780, doi:10.1073/pnas.0705006105

Huertas, I. E., B. Colman, and G. S. Espie. 2002. Mitochondrial-driven bicarbonate transport supports photosynthesis in a marine microalga. Plant Physiol. **130:** 284–291, doi:10.1104/pp.004598

Hutchins, D. A., and others. 2007. CO_2 control of *Trichodesmium* N_2 fixation, photosynthesis, growth rates, and elemental ratios: Implications for past, present, and future ocean biogeochemistry. Limnol. Oceanogr. **52:** 1293–1304.

Jeffrey, S. W., and S. W. Wright. 1994. Photosynthetic pigments in the Haptophyta, p. 111–132. *In* J. C. Green and B. S. C. Leadbeater [eds.], The Haptophyte algae. Clarendon Press.

Kaplan, A., and L. Reinhold. 1999. CO_2 concentrating mechanisms in photosynthetic microorganisms. Ann. Rev. Plant Physiol. Plant Mol. Biol. **50:** 539–570, doi:10.1146/annurev.arplant.50.1.539

Kolber, Z. S., O. Prasil, and P. G. Falkowski. 1998. Measurements of variable chlorophyll fluorescence using fast repetition rate techniques: Defining methodology and experimental protocols. Biochim. Biophys. Acta **1367:** 88–106, doi:10.1016/S0005-2728(98)00135-2

Landry, M. R., J. Constantinou, M. Latasa, S. L. Brown, R. R. Bidigare, and M. E. Ondrusek. 2000. Biological response to iron fertilization in the eastern equatorial Pacific (IronEx II). III. Dynamics of phytoplankton growth and microzooplankton grazing. Mar. Ecol. Prog. Ser. **201:** 57–72, doi:10.3354/meps201057

Levitan, O., and others. 2007. Elevated CO_2 enhances nitrogen fixation and growth in the marine cyanobacterium *Trichodesmium*. Glob. Change Biol. **13:** 531–538, doi:10.1111/j.1365-2486.2006.01314.x

Lueker, T. J., A. G. Dickson, and C. D. Keeling. 2000. Ocean pCO_2 calculated from dissolved inorganic carbon, alkalinity, and equations for K1 and K2: Validation based on laboratory measurements of CO_2 in gas and seawater at equilibrium. Mar. Chem. **70:** 105–119, doi:10.1016/S0304-4203(00)00022-0

Martin, J. H., and S. E. Fitzwater. 1988. Iron-deficiency limits phytoplankton growth in the northeast Pacific Subarctic. Nature **331:** 341–343, doi:10.1038/331341a0

McGinn, P. J., and F. M. M. Morel. 2008. Expression and regulation of carbonic anhydrases in the marine diatom *Thalassiosira pseudonana* and in natural phytoplankton assemblages from the Great Bay, New Jersey. Physiol. Plant. **133:** 78–91, doi:10.1111/j.1399-3054.2007.01039.x

Morel, F. M. M. 1987. Kinetics of nutrient-uptake and growth in phytoplankton. J. Phycol. **23:** 137–150.

Parsons, T. R., Y. Maita, and C. M. Lalli. 1984. A manual of chemical and biological methods for seawater analysis. Pergamon.

Raven, J. A. 1990. Predictions of Mn and Fe use efficiencies of phototrophic growth as a function of light availability for growth and of C assimilation pathway. New Phytol. **116:** 1–18, doi:10.1111/j.1469-8137.1990.tb00505.x

———. 1991. Physiology of inorganic C acquisition and implications for resource use efficiency by marine phytoplankton: Relation to increased CO_2 and temperature. Plant Cell Environ. **14:** 779–794, doi:10.1111/j.1365-3040.1991.tb01442.x

Reinfelder, J. R., A. M. L. Kraepiel, and F. M. M. Morel. 2000. Unicellular C_4 photosynthesis in a marine diatom. Nature **407:** 996–999, doi:10.1038/35039612

Riebesell, U., D. A. Wolf-Gladrow, and V. Smetacek. 1993. Carbon dioxide limitation of marine phytoplankton growth rates. Nature **361:** 249–251, doi:10.1038/361249a0

———, I. Zondervan, B. Rost, P. D. Tortell, R. E. Zeebe, and F. M. M. Morel. 2000. Reduced calcification of marine phytoplankton in response to increased atmospheric CO_2. Nature **407:** 364–367, doi:10.1038/35030078

———, and others. 2007. Enhanced biological carbon consumption in a high CO_2 ocean. Nature **450:** 545–548, doi:10.1038/nature06267

Ross, S. M. 2007. Introduction to probability models, 9th ed. Academic Press.

Rost, B., U. Riebesell, S. Burkhardt, and D. Sultemeyer. 2003. Carbon acquisition of bloom-forming marine phytoplankton. Limnol. Oceanogr. **48:** 55–67.

Saez, A. G., I. Probert, J. R. Young, B. Edvardsen, W. Eikrem, and L. K. Medlin. 2004. A review of the phylogeny of the Haptophyta. *In* H. R. Thierstein and J. R. Young [eds.], Coccolithophores: From molecular processes to global impact. Springer.

Scott, K. M., M. Henn-Sax, T. L. Harmer, D. L. Longo, C. H. Frame, and C. M. Cavanaugh. 2007. Kinetic isotope effect and biochemical characterization of form IA RubisCO from the marine cyanobacterium *Prochlorococcus marinus* MIT9313. Limnol. Oceanogr. **52:** 2199–2204.

Shi, D., Y. Xu, B. M. Hopkinson, and F. M. M. Morel. 2010. Effect of ocean acidification on iron availability to marine phytoplankton. Science **327:** 676–679, doi:10.1126/science.1183517

Smith, F. A., and J. A. Raven. 1979. Intracellular pH and its regulation. Ann. Rev. Plant Physiol. **30:** 289–311, doi:10.1146/annurev.pp.30.060179.001445

Strzepek, R. F., and P. J. Harrison. 2004. Photosynthetic architecture differs in coastal and oceanic diatoms. Nature **431:** 689–692, doi:10.1038/nature02954

Sultemeyer, D. F., H. P. Fock, and D. T. Canvin. 1991. Active uptake of inorganic carbon by *Chlamydomonas reinhardtii*: Evidence for simultaneous transport of HCO^-_3 and CO_2 and characterization of active CO_2 transport. Can. J. Bot. **69:** 995–1002, doi:10.1139/b91-128

Sunda, W. G., and S. A. Huntsman. 1997. Interrelated influence of iron, light and cell size on marine phytoplankton growth. Nature **390:** 389–392, doi:10.1038/37093

Tamura, K., J. Dudley, M. Nei, and S. Kumar. 2007. MEGA4: Molecular evolutionary genetic analysis (MEGA) software version 4.0. Mol. Biol. Evol. **24:** 1596–1599, doi:10.1093/molbev/msm092

Tortell, P. D., G. H. Rau, and F. M. M. Morel. 2000. Inorganic carbon acquisition in coastal Pacific phytoplankton

communities. Limnol. Oceanogr. **45:** 1485–1500, doi:10.4319/lo.2000.45.7.1485

———, AND OTHERS. 2008. CO_2 sensitivity of Southern Ocean phytoplankton. Geophys. Res. Lett. **35:** L04605, doi:10.1029/2007GL032583

TWINING, B. S., S. B. BAINES, N. S. FISHER, AND M. R. LANDRY. 2004. Cellular iron contents of plankton during the Southern Ocean Iron Experiment. Deep-Sea Res. I **51:** 1827–1850, doi:10.1016/j.dsr.2004.08.007

WELSCHMEYER, N. A. 1994. Fluorometric analysis of chlorophyll *a* in the presence of chlorophyll *b* and pheopigments. Limnol. Oceanogr. **39:** 1985–1992, doi:10.4319/lo.1994.39.8.1985

ZHANG, H., AND R. H. BYRNE. 1996. Spectrophotometric pH measurements of surface seawater at in-situ conditions: Absorbance and protonation behavior of thymol blue. Mar. Chem. **52:** 17–25, doi:10.1016/0304-4203(95)00076-3

Associate editor: Everett Fee

Received: 29 December 2009
Accepted: 26 May 2010
Amended: 10 June 2010